 

PACS numbers: 42.30.Wb; 42.25.Fx
DOI: 10.1070/QE2006v036n03ABEH013130

# Effect of photons of different scattering orders on the formation of a signal in optical low-coherence tomography of highly scattering media

M.Yu. Kirillin, I.V. Meglinski, A.V. Priezzhev

***Abstract*. The influence of photons of different scattering orders on the formation of a detected signal in optical low-coherence tomography (OCT) is considered. The scattering orders are estimated by analysing the spatial distribution of the probability density for the effective optical paths of detected photons calculated by the Monte Carlo method. The influence of photons with different scattering orders on the formation of a signal is estimated quantitatively depending on the optical properties of the medium under study. The results of numerical simulations are interpreted within the framework of possible applications of OCT for non-invasive diagnostics of the human skin and other highly scattering random media. It is shown by the example of calculation of OCT signals from model biological tissues that the OCT method gives reliable information on their internal structure from optical depths up to 0.3 mm.**

***Keywords***: *optical low-coherence tomography, Monte Carlo method, multiple scattering, low-order scattering.*

## 1. Introduction

The methods of optical non-invasive diagnostics being actively developed beginning from the mid-1980s [1] are widely used today in various fields of medicine and biophysics [2, 3]. One of the most promising methods, which is successfully applied for diagnostics of the human eyeground, mucosa, monitoring of morphological variations in the cutaneous covering, etc., is optical low-coherence tomography (OCT) [4, 5].* The OCT method provides the imaging of the internal structure of biological tissues with a rather high spatial resolution (2 – 15 μm) [5 – 9]. The maximum visualisation depth is limited by the contribution from multiply scattered photons, which increases with depth, and is comparable with the transport mean free path of photons $l_{tr} = (\mu_a + \mu_s')^{-1}$. Here, $\mu_s' = \mu_s(1 - g)$ is the so-called reduced scattering coefficient; $\mu_s$ is the scattering coefficient; $\mu_a$ is the absorption coefficient; and $g$ is the anisotropy factor, which is equal to the mean cosine of the scattering angle. In this connection the most promising is the use of OCT for visualisation of superficial layers of biological tissues. It is obvious that the maximum OCT visualisation depth can be increased, under the condition that high spatial resolution is preserved, by increasing $l_{tr}$ and (or) decreasing the contribution of multiply scattered photons to a detected signal.

In practice, the value of $l_{tr}$ can be increased by using the diffusion of osmotic substances into a biological tissue [10]. At present this is one of the most promising directions of studies in biomedical optics [3, 9 – 12]. In turn, the influence of multiply scattered photons can be reduced and the role of low-order scattered photons in the detected signal can be increased by using a special optical scheme, for example, by the conjugate diaphragming of an objective and the field of detector with the so-called narrow-transmission collimators [13, 14].

Hereafter, we will consider the two classes of detected photons: multiply scattered (MS) and low-order scattered (LOS) photons. For photons of the first class the difference between their optical path $l$ in a medium and the doubled maximal optical depth $2z_{max}$ achieved in the medium exceeds the coherence length $l_{coh}$ of a source:

$$l - 2z_{max} > l_{coh}. \quad (1)$$

In this case, it is assumed that detected photons give distorted information on the position of scatterers (structural elements of the tissue) [15]. Photons for which inequality (1) is not fulfilled belong to LOS photons carrying useful information on the distribution of optical inhomogeneities in the medium.

The aim of this paper is to study the dependence of a detected OCT signal on the contributions of photons with

**M.Yu. Kirillin** Department of Physics, M.V. Lomonosov Moscow State University, Vorob'evy gory, 119992 Moscow, Russia; University of Oulu, Faculty of Technology, Optoelectronics and Measurement Techniques Laboratory. P.O. Box 4500, 90014, Oulu, Finland; e-mail: mkirillin@yandex.ru;
**I.V. Meglinski** N.G. Chernyshevskii Saratov State University, ul. Moscovskaya 155, 410026 Saratov, Russia; present address: Cranfield University, School of Engineering, Cranfield, MK43 0AL, UK; e-mail: i.meglinski@cranfield.ac.uk;
**A.V. Priezzhev** Department of Physics, International Laser Center, M.V. Lomonosov Moscow State University, Vorob'evy gory, 119992 Moscow, Russia; e-mail: avp2@mail.ru

Received 3 November 2005
*Kvantovaya Elektronika* **36** (3) 247 – 252 (2006)
Translated by M.N. Sapozhnikov

*This method is a refined variant of optical low-coherence interferometry [6, 7] and (or) optical low-coherence reflectometry [8]. It is based on the use of a low-coherence optical radiation source in a Michelson interferometer. Nevertheless, we employ the abbreviation OCT in accordance with the accepted term Optical Coherence Tomography.

different scattering orders. This problem attracts recent attention [15–21] in connection with the search for possibilities of separating LOS photons from the total detected signal or increasing their contribution to the latter [19, 20]. It is this type of photons that gives information on the positions of scatterers in a volume being probed.

In this paper, we selected photons according to the above classification by the Monte Carlo (MC) method and estimated the contributions from photons of two types to the detected signal. The results were interpreted within the framework of possible applications of OCT for studying highly scattering anisotropic media, for example, blood and skin.

## 2. Principles of optical coherence tomography

The principles and various applications of OCT were considered in detail in many papers (see, for example, [5, 9] and references therein). As in the case of confocal microscopy [22, 23], the tomograph uses the conjugate diaphragming of a low-coherent radiation source and the field of view of the photodetector by means of diaphragms placed in the object and image planes (Fig. 1).

Such a conjugation restricts the size of the central focal spot formed by a focusing optical system. As a result, this optical system allows one to localise measurements within a small volume of $8-50\ \mu m^3$, which was clearly demonstrated in [12]. This scheme in combination with a Michelson interferometer provides a rapid scan over the object depth (along the coordinate $z$) by the uniform movement of a mirror in the reference arm of the interferometer (Fig. 1). In this case, the amplitude of the detected signal changes proportionally to changes in the refractive index corresponding to the position of the structural elements of the tissue at the probe depth.

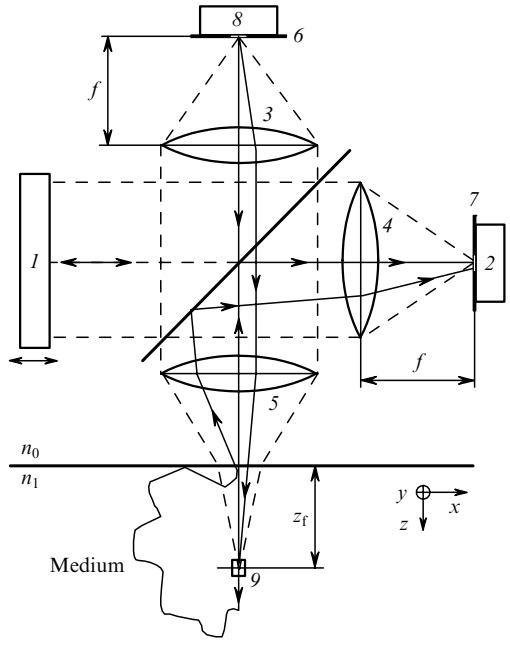


**Figure 1.** Scheme of the OCT method: (*1*) movable mirror in the reference arm of an interferometer (a medium under study is located in the object arm); (*2*) photodetector measuring the interference signal obtained after optical mixing of waves coming from the object and reference arms; (*3*, *4*, *5*) short-focus lenses forming in pairs a narrow-transmission collimator; (*6*, *7*) diaphragms; (*8*) low-coherence radiation source (superluminescent laser diode or femtosecond laser); (*9*) localisation region of the probe radiation ($8-50\ \mu m^3$); $z_f$ is the depth of the focal point inside a medium; $f$ is the focal distance of the lens.

Therefore, the dependence of the signal amplitude on the scan time gives information on the distribution of optical microinhomogeneities over the depth. Under typical experimental conditions, the OCT method allows one to obtain the image of the cell structure of human skin (i.e., to distinguish LOS photons against the background of all scattered photons) at depths up to 1–2 mm [5, 9].

The most important parameter of an optical coherence tomograph is its spatial resolution $\Delta z$ over the depth, which is determined by the spectral width of a low-coherence laser

$$\Delta z = \frac{2\ln 2}{\pi}\,\frac{\lambda_c^2}{\Delta\lambda}. \tag{2}$$

Here, $\lambda_c$ and $\Delta\lambda$ are the central wavelength and half-width of the laser spectrum, respectively. The distance $\Delta z$ is also determined by the width of the coherence function of the laser and is called its coherence length $l_{coh}$. For example, for a 820-nm superluminescent laser diode (SLD) with $\Delta\lambda = 20$ nm, we have $\Delta z \approx 15\ \mu m$ [24]. Such a high spatial resolution is achieved due to localisation of probe low-coherence ($l_{coh} \sim 10-20\ \mu m$) radiation within a small volume and the heterodyne mixing of the reference and probe signals. The spatial resolution of OCT systems is improved when broadband radiation sources are used.

## 3. Monte Carlo calculations of scattering orders

One of the most efficient methods for qualitative and quantitative estimating the effect of different scattering orders on the formation of the OCT signal is statistical MC simulations [16–20, 25]. Note that the intensity of radiation scattered in random media is calculated in the MC method by the direct summation of series in scattering orders [26]. This method allows one to take into account the structure of biological tissues, the parameters of an experimental setup, the size and shape of the incident beam, multiple reflection from interfaces between medium layers of different shapes, interference effects, and other parameters [12, 18, 24–28]. With the properly selected parameters of the medium under study, the MC method can reproduce quite accurately the reflection spectrum of the human skin [27].

We determined the OCT signal by calculating the optical paths of photons in the object and reference arms by the MC method [16, 18–20] (Fig. 1). The model signal was calculated as a superposition of partial interference signals from the obtained distribution of optical paths taking into account the coherence function of the low-coherence source from the expression

$$I(t) = \sum_{\Delta l} [N_r N_s(t,\Delta l)]^{1/2} \cos\left(\frac{2\pi}{\lambda}\,\Delta l\right) \times \exp\left[-\left(\frac{\Delta l}{l_{coh}}\right)^2\right], \tag{3}$$

where $N_r(t,\Delta l)$ and $N_s(t,\Delta l)$ are the number of photons coming from the reference and object arms, respectively; and $\Delta l$ is their path difference [5].

We assumed in calculations that the coherence function of the SLD is Gaussian with the width $l_{coh} = 15$ μm and the probe-beam waist is located on the surface of the object under study. This corresponds to the real parameters of a broadband radiation source and experimental conditions [24]. The trajectories of light photons in blood and intralipid were calculated by using the Henyey–Greenstein phase scattering function, which was earlier successfully employed in simulations of light propagation in biological tissues [2, 3]:

$$f_{HG}(\theta) = \frac{1}{4\pi} \frac{1 - g^2}{(1 + g^2 - 2g\cos\theta)^{3/2}}, \quad (4)$$

where $\theta$ is the polar scattering angle. The azimuthal distribution over the angle $\varphi$ was assumed uniform. To increase the efficiency of the MC method, we used the scheme of the so-called implicit capture of absorption. In this scheme, not one but a group (packet) of photons, which is characterised by some weight, propagates along each random path [26–28]. This approach allows one to take simply into account the absorption and repeated reflections from interfaces in the medium and considerably reduces the calculation time, by preserving the accuracy of calculations [27, 28]. We obtained one model signal (scan over the depth) by calculating the propagation of $5 \times 10^7$ photon packets.

The principal feature of the method used in our paper is the abandonment of the 'Russian roulette' procedure employed in [15, 17]. This procedure is applied to equalise the energy balance of the incident radiation, radiation absorbed by the medium and that escaped from the region under study due to scattering. This is achieved by periodically increasing the statistical weight of randomly selected photon packets at the expense of photons excluded from further consideration because of their small statistical weight or escape beyond the medium boundaries. This increase in the statistical weight raises the chance that a photon will leave the medium at the detection point. In this case, however, a groundless increase in the optical path of a photon occurs, which can lead to erroneous results in the calculation of the distribution of optical paths of photons.

We considered single- and multilayer model media. The parameters of layers were selected in accordance with typical optical parameters of blood (treated as a suspension of non-aggregated erythrocytes) and the 2-% intralipid solution. Intralipid is a polydispersed suspension of nearly spherical scattering particles with the average size ~ 0.3-μm suspended in the glycerol–water solution. The scattering particles are droplets of soy oil covered by a thin (2.5–5.0 nm) lecithin membrane [27, 29, 30]. Intralipid is often used in optical experiments to simulate skin because their optical properties in the near-IR region are close [2, 3, 31]. The optical parameters used in simulations are presented in Table 1.

**Table 1.** Optical parameters used in simulations ($\lambda = 820$ nm).

| Medium | $\mu_s/\text{mm}^{-1}$ | $\mu_a/\text{mm}^{-1}$ | $g$ | $n$ | $l_{tr}$/mm | References |
|---|---|---|---|---|---|---|
| Blood (35 % hematocrit) | 57.3 | 0.82 | 0.977 | 1.35 | 0.468 | [32] |
| 2-% intralipid solution | 5.4 | 0.0004 | 0.63 | 1.35 | 0.5 | [29, 30] |

## 4. Results and discussion

Figure 2 shows the typical model OCT signal from a 0.5-mm thick layer of a scattering medium in air. The optical parameters of the layer (Table 1) were selected close to those of blood [2, 3, 32].

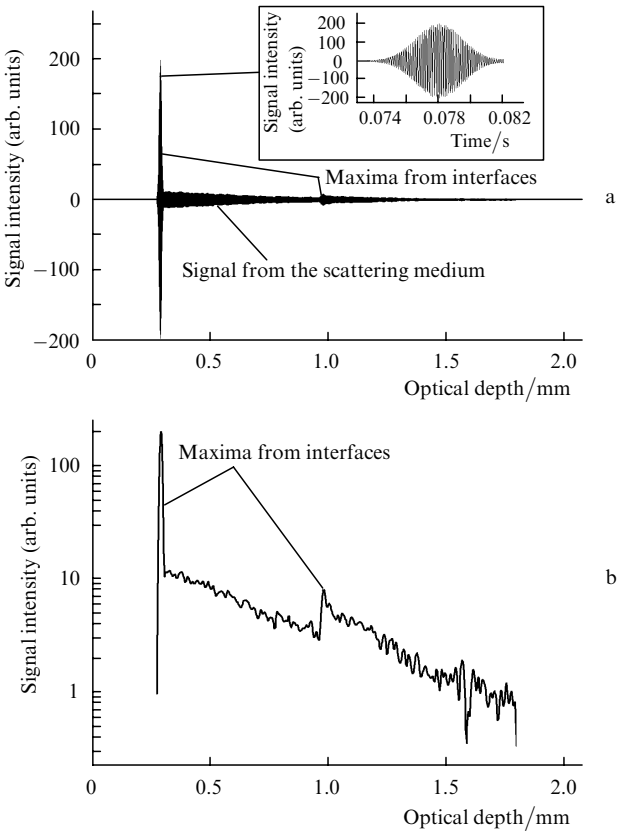


**Figure 2.** Typical time sweep of the OCT signal from a blood layer: interference signal from the front interface (insert) at a linear scale (a) and the envelope of the OCT signal at a semi-logarithmic scale (b).

Figure 2a presents a sweep of the detected OCT signal, and Fig. 2b shows the envelope of this signal presented at the semi-logarithmic scale. One can easily see that the pronounced peaks correspond to the boundaries of the layer under study at which the mismatch of the refractive index occurs. The signal between peaks corresponds to a homogeneous medium and its shape is determined by the optical properties of the medium. After the second peak, the signal follows which corresponds to photons coming from the depth exceeding the layer thickness and is determined exclusively by multiple scattering.

The envelopes of model signals from intralipid and blood layers of thickness 1 mm each (the corresponding optical thickness is 1.35 mm) and the contributions from MS and LOS photons are presented in Figs 3 and 4. One can see that in the case of intralipid (Fig. 3), the signal contains two characteristic peaks corresponding to the layer boundaries. In the case of blood (Fig. 4), the rear boundary of the layer is not observed because of a stronger scattering than in intralipid. For the same reason, a stronger decrease in the contribution of LOS photon with increasing depth is observed. The maximum localisation depth of the probe radiation can be estimated from the criterion for the

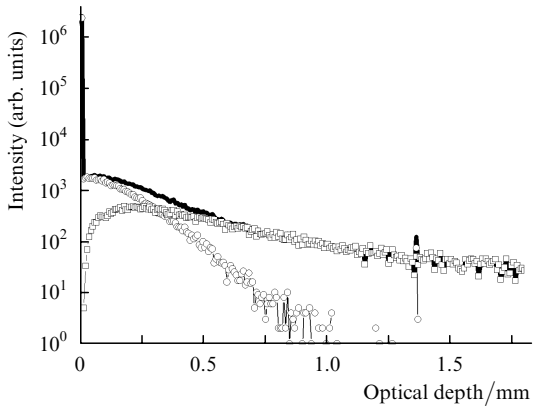


**Figure 3.** Envelope of the model OCT signal (thick curve) and contributions of LOS (○) and MS (□) photons as functions of the probe depth of the intralipid layer.

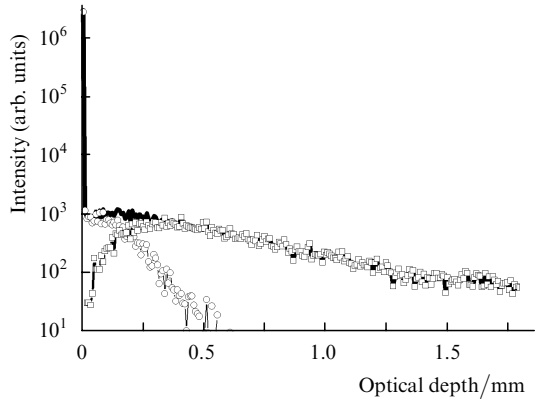


**Figure 4.** Envelope of the model OCT signal (thick curve) and contributions of LOS (○) and MS (□) photons as functions of the probe depth of the erythrocyte-suspension layer.

predominance of LOS photons in the total detected signal [15–17]. Therefore, this depth can be estimated in this case from the condition of the equality of contributions from MS and LOS photons. It follows from the results obtained that the maximum optical localisation depth for a homogeneous intralipid layer is 0.3 mm and for a homogeneous blood layer is 0.2 mm, in good agreement with experiments [33].

Figure 5 shows the contributions from photons of different scattering orders to the OCT signal calculated as functions of the depth of probing intralipid and erythrocyte-suspension layers presented in Figs 3 and 4, respectively. These results well agree with the data obtained in [15, 17]. Note that the dependence of the contribution of single scattering on the optical depth is qualitatively the same for intralipid and erythrocyte suspension, whereas contributions from higher scattering orders are substantially different. Hereafter, we call the optical depth the physical depth multiplied by the corresponding refractive index of each layer.

Figure 6 presents the dependences of the ratio of contributions from photons of different scattering orders for the erythrocyte suspension layer to contributions for the intralipid layer on the probe depth. Note that, although the scattering coefficients of these model media differ by an order of magnitude (see Table 1), a pronounced correlation is observed in the relation of scattering orders (Fig. 6).

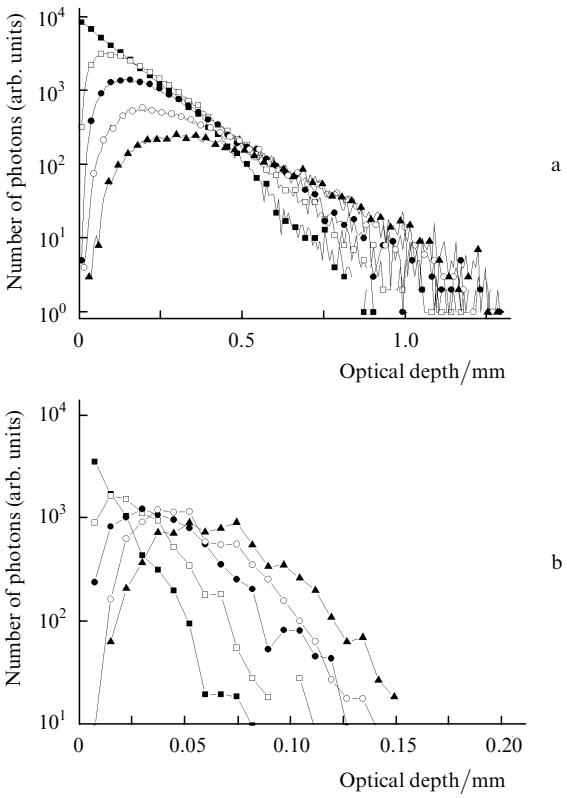


**Figure 5.** Contributions of the first and fifth scattering orders to the OCT signal as functions of the probe depth of the intralipid (a) and erythrocyte-suspension (b) layers. Points ■, □, ●, ○, and ▲ correspond to the first–fifth scattering orders, respectively.

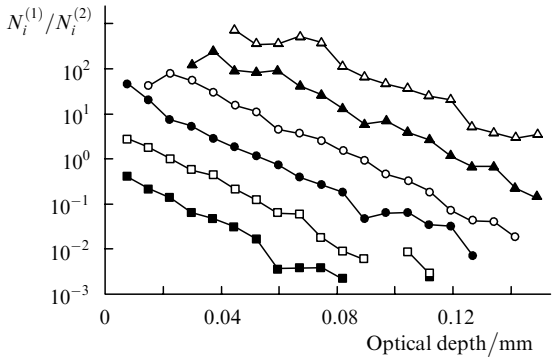


**Figure 6.** Ratios of the contributions $N_i^{(1)}(z)$ of photons of different scattering orders for the erythrocyte-suspension layer to contributions $N_i^{(2)}(z)$ for the intralipid layer as functions of the probe depth. Points ■, □, ●, ○, ▲ and △ correspond to the first–sixth scattering orders, respectively.

We also studied the dependences of contributions from the LOS and MS components to different parts of the OCT signal for multilayer media. Figure 7 shows typical results of simulations for a three-layer model of the biological tissue consisting of two layers of the 2 % intralipid and a blood layer between them. The thickness of the surface intralipid layer is 50 μm (the optical thickness is 67.5 μm) and the thickness of the blood layer is 100 μm (the optical thickness is 135 μm) and the thickness of the deep intralipid layer is 850 μm (the optical thickness is 1147.5 μm). The model OCT signal exhibits distinct peaks corresponding to the boundaries of the blood layer. The decrease in the signal

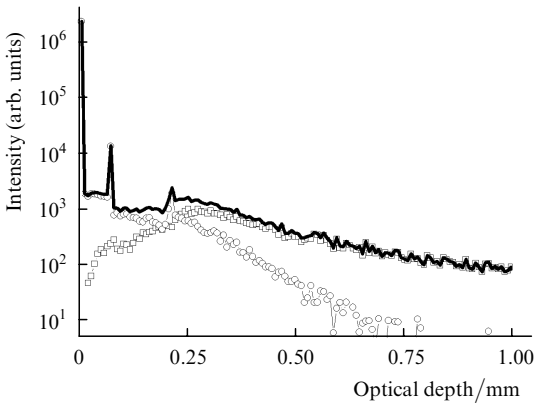


**Figure 7.** Model OCT signal (thick curve) and contributions of LOS (□) and MS (○) photons for the three-layer optical model (the thickness of the upper intralipid layer is 50 μm, the thickness of the blood layer is 100 μm).

intensity in the region corresponding to the blood layer (between the peaks) is explained by a higher scattering anisotropy in blood compared to intralipid.

Note that the peaks corresponding to the boundaries of the blood layer are mainly formed by LOS photons, whereas the contribution of MS photons has no pronounced levels corresponding to the boundaries. One can also see from Fig. 7 that multiple scattering dominates in the signal at optical depths exceeding 0.25 mm, in accordance with the estimates obtained for homogeneous layers.

The thickness of the surface intralipid layer in our three-layer model (the depth of position of the blood layer) was varied from 50 to 300 μm (the optical depth was varied from 67.5 to 405 μm). The dependences of the contributions of LOS and MS photons to different parts of the signal on the blood layer position are presented in Fig. 8. The results show that LOS photons dominate in the part of the signal corresponding to the first intralipid layer, their contribution increasing with the layer thickness. LOS photons also dominate in the signal from the first boundary of the blood layer; however, their contribution considerably decreases with increasing the depth of position of the layer interface (with increasing the number of MS photons). The decrease in the LOS component of the signal with increasing the first-layer depth is explained by strong scattering in the first layer. As a result, the number of photons propagated to deeper layers and backscattered from these layers decreases. Note also that, although for depths of layers exceeding 0.2 mm, MS photons dominate in the part of the signal from the blood layer, the signal from the second boundary of the layer (second peak) is formed by LOS photons, as pointed out earlier. We obtained similar results for a five-layer model of the skin. They are not presented here because of their qualitative coincidence with the results obtained for the three-level model.

The results obtained for multilayer models confirm the data on the limiting detection and localisation depths of internal inhomogeneities obtained for homogeneous blood and intralipid layers. However, it should be noted that this is valid for optically soft inhomogeneities ($n < 1.05$) typical for biological tissues [2]. Harder inhomogeneities (such as the

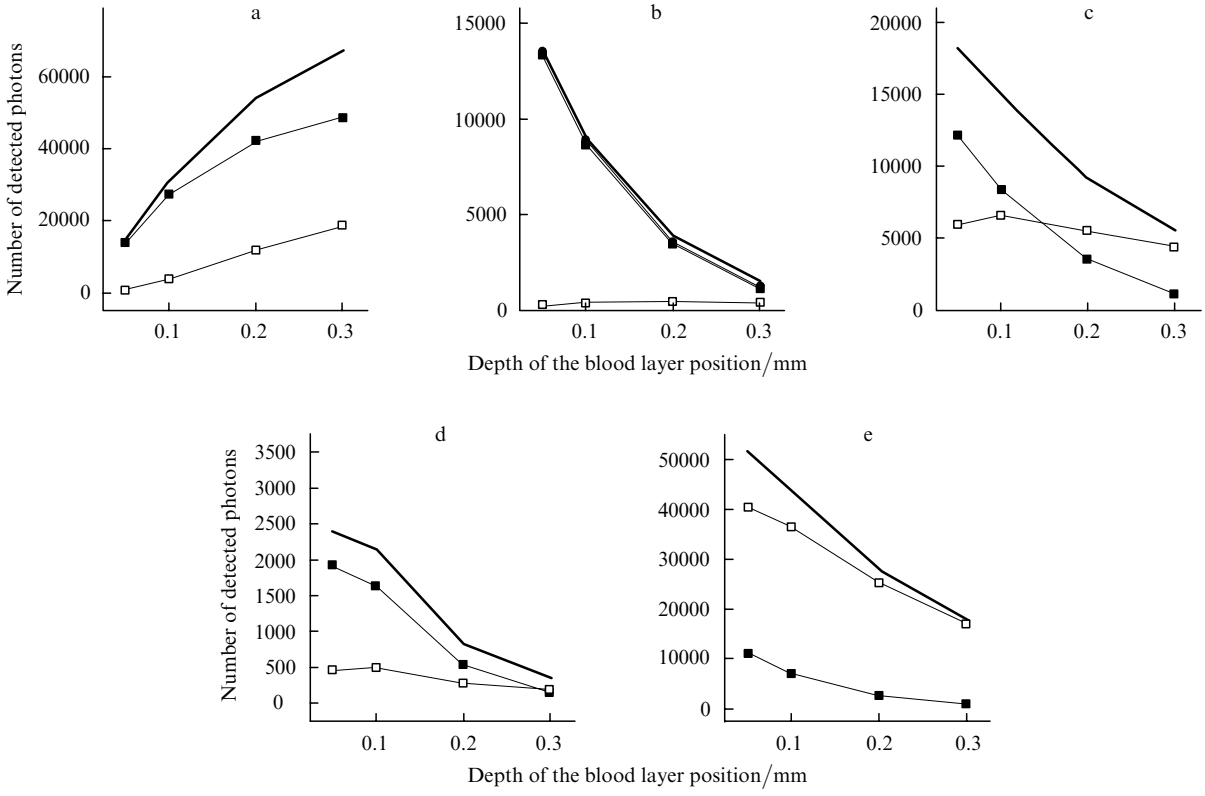


**Figure 8.** Contributions of different components [(thick curve) all photons; ■ LOS photons; □ MS photons] to different parts of the model OCT signal from the three-layer skin model [(a) from the first intralipid layer; (b) from the intralipid – blood interface; (c) from the blood layer; (d) from the blood – intralipid interface; (e) from the second intralipid layer].

rear boundary of the intralipid layer) can be detected at greater depths.

## 5. Conclusions

We have analysed the contributions of photons of different scattering orders to the OCT signal and presented the results of Monte Carlo simulation of highly scattering homogeneous and multilayer media. The optical properties of the layers of the model medium were selected close to those of human blood and skin.

It has been shown that the contribution of single scattering to the OCT signal remains qualitatively the same with increasing the optical depth. The contributions of photons of higher-order scattering orders demonstrate the quantitative correlation despite the increase in the scattering coefficient by an order of magnitude. This can be explained by the fact that the instrumental function is the same in both cases. These results agree indirectly with the data obtained in [20, 34].

It has been shown that the OCT method provides good resolution upon visualisation of the internal structure of objects at depths up to 0.3 mm, which is determined by the dominant role of multiple scattering at these depths. The maximum optical localisation depth of optical radiation was 0.3 mm for the homogeneous intralipid layer and 0.2 mm for the homogeneous blood layer.

These results well agree with theoretical [15, 17] and experimental [33] data, which allows their interpretation within the framework of OCT studies of human skin and other biological tissues.

***Acknowledgements.*** This work was supported by the UK Biotechnology and Biology Scientific Research Council (Grant No. BBS/B/04242), the GETA Graduate School (Finland), and partially by the Program Leading Scientific Schools of Russia (Grant No. 2071.2003.4), the Royal Society (Grant No. 152987), and NATO (Grant No. PST.CLG. 979652).

## References

1. Priezzhev A.V., Tuchin V.V., Shubochkin L.P. *Lazernaya diagnostika v biologii i meditsine* (Laser Diagnostics in Biology and Medicine) (Moscow: Nauka, 1989).
2. Tuchin V.V. *Lazery i volokonnaya optika v biomeditsinskikh issledovaniyakh* (Lasers and Fibre Optics in Biomedical Studies) (Saratov: Izd. Saratov. Univer., 1998).
3. Tuchin V.V. (Ed.). *Handbook of Optical Biomedical Diagnostics* (Bellingham: SPIE Press, 2002).
4. Huang D. et al. *Science*, **254**, 1178 (1991).
5. Bouma B.E., Tearney G.J. (Eds) *Handbook of Optical Coherence Tomography* (New York: Marcel Dekker, 2002).
6. Linnik V.P. *Trudy Akad. Nauk SSSR*, **1**, 208 (1933).
7. Flourney P.A. *Appl. Opt.*, **11**, 1907 (1972).
8. Gilgen H.H. et al. *J. Lightwave Technol.*, **7**, 1225 (1989).
9. Tuchin V.V. (Ed.) *Coherent-Domain Optical Methods: Biomedical Diagnostics, Environmental and Material Design* (Boston: Kluwer Academic Publishers, 2004) Vol. 2.
10. Tuchin V.V. et al. *J. Biomed. Opt.*, **2**, 401 (1997).
11. Vargas G. et al. *Lasers Surg. Med.*, **24**, 133 (1999).
12. Meglinski I.V. et al. *Kvantovaya Elektron.*, **32**, 875 (2002) [*Quantum Electron.*, **32**, 875 (2002)].
13. Inoue S., Spring K.R., in *Video Microscopy. The Fundamentals* (New York: Plenum Press, 1997) pp 13–117.
14. Webb R.H. *Rep. Prog. Phys.*, **59**, 427 (1996).
15. Wang R.K. *Phys. Med. Biol.*, **47**, 2281 (2002).
16. Bykov A.V., Kirillin M.Yu., Priezzhev A.V. *Kvantovaya Elektron.*, **35**, 135 (2005) [*Quantum Electron.*, **35**, 135 (2005)].
17. Yao G., Wang L.V. *Phys. Med. Biol.*, **44**, 2307 (1999).
18. Kirillin M.Yu., Priezzhev A.V. *Kvantovaya Elektron.*, **32**, 883 (2002) [*Quantum Electron.*, **32**, 883 (2002)].
19. Meglinski I.V. et al. *Laser Phys. Lett.*, **1**, 387 (2004).
20. Berrocal E. et al. *Appl. Opt.*, **44**, 2519 (2005).
21. Gelikonov G.V. et al. *Izv. Vyssh. Uchebn. Zaved., Ser. Radiofiz.*, **46**, 628 (2003).
22. Wilson T. *Confocal Microscopy* (San Diego: Academic Press, 1990).
23. Pawley J.B. *Handbook of Biological Confocal Microscopy* (New York: Plenum Press, 1995).
24. Kirillin M. et al. *Proc. SPIE Int. Soc. Opt. Eng.*, **5325**, 164 (2004).
25. Yaroslavsky I.V., Tuchin V.V. *Opt. Spektr.*, **72**, 934 (1993).
26. Meglinski I.V. et al. *Proc. Roy. Soc. A*, **461**, 43 (2005).
27. Meglinski I.V., Matcher S.J. *Physiol. Meas.*, **23**, 741 (2002).
28. Churmakov D.Y. et al. *Phys. Med. Biol.*, **47**, 4271 (2002).
29. Flock S.T. et al. *Lasers Surg. Med.*, **12**, 510 (1992).
30. Van Staveren H.J. et al. *Appl. Opt.*, **30**, 4507 (1991).
31. Troy T.L., Thennadil S.N. *J. Biomed. Opt.*, **6**, 167 (2001).
32. Roggan A. et al. *J. Biomed. Opt.*, **4**, 36 (1999).
33. Kuranov R.V. et al. *Opt. Express*, **10**, 707 (2002).
34. Berrocal E. et al. *Proc. SPIE Int. Soc. Opt. Eng.*, **5771**, 74 (2005).